Chapter 4

A Meandered Inductive Loop based RFID Tag Antenna For Luggage Tracking

4.1 Introduction

In 1999, United States' Uniform Code Council (UCC) and European Article Numbering Association (EAN), presently both known as GS1, launched an Auto-ID center in Ultra High Frequency band for developing Electronic Product Code (EPC)[3]. In UHF Radio frequency identification technology, tag receives power from incoming electromagnetic waves evolving from the reader and back-scatters the signal on the way to reader. The evolution in semiconductor market in 1990s expedited the RFID-commercialization in transportation, logistics, supply chain supervision and product tracing. In recent past years, RFID has been victorious in superseding other automatic identification techniques like barcodes, smart cards and magnetic stripe cards, because of its advantage of providing non-line of sight connection with considerable storage. At present, Radio Frequency Identification (RFID) methodology has been accomplishing its peak in area of Hospitals, Electronic Payment Systems, Libraries, Access control, Agriculture, , Marathons and

many more applications[61].

In 2002, FCC (Federal Communications Commission) accredited Ultra Wide Band Radio Frequency Identification for wholesale applications and sanctioned various frequency bands for RFID applications. The four different frequency bands for RFID have already been discussed in Section 2.3. The Ultra-high frequency band i.e. 860 to 960 MHz RFID devices have been more preferred correlated to LF and HF entities because they can be able to operate for more miniaturized antennas and empower simultaneous exposure of collective tags[62]. A certain country or territory has been designated limited frequency band.

The eminent Ultra High Frequency RFID tags exibits higher read territory albeit need of lower transmission power. The semiconductor-chip used in UHF tag is data storing device and capacitive in nature. For complex impedance matching with semiconductor-chip, inductive tag antenna is used. In [63], Yao *et.al.* presents multi-polarized RFID antenna and show how a meandering microstrip open-ended lines can be used for near-field applications. The inductance as well as the resonating frequency of meander line dipole antenna is adjusted by tuning the height of meander-line, its length and number of meanders[64]. The equivalent circuit analysis of inductively coupled loop based RFID tag for on-body application is explained in [65]. Among all of these designed antennas, it is found that meander line antenna is befitting for Ultra High Frequency RFID applications because of its good inductive reactance, planar geometry and miniaturized size.

This chapter presents a comprehensive analysis of a meander line RFID tag with spiral-ending coupled with two-sided Meandered Inductive Loop (MIL). Inductive-coupled loop is used for impedance matching while meandering technique is used for contraction of antenna dimensions. Hence this hybridization produces the novelty of proposed RFID tag antenna with tiny size and better reading territory. Here, it works at 866 MHz which lies in the UHF band of India for RFID applications. It is comprehended from this chapter that this antenna has adequate reading territory and compactness with respect to size contrary to erstwhile designs. Here, tag input impedance matching with semiconductor-chip Alien(Higgs-4) SOT, equivalent circuit prototype of tag, reflection coefficient and

reading territory are presented. This proposed tag was designed and simulated with High Frequency Structure Simulator of Ansys-2020R1 software.

4.2 Proposed UHF Tag

The graphics of the proposed antenna is displayed in Figure 4.1. The tag has trace of $60mm \times 16mm \times 1.6mm$ built on FR4 glass epoxy substrate (ϵ_r=4.4, tanδ=0.02) having thickness of 1.6 mm. This antenna is designed with meandering technique for size contraction. The tag antenna is consisting a symmetric double sided Meandered Inductive Loop(MIL) microstrip dipole providing remarkable impedance matching with semiconductor-chip.

The resonating frequency is changed by alternating the spiral length, meander line

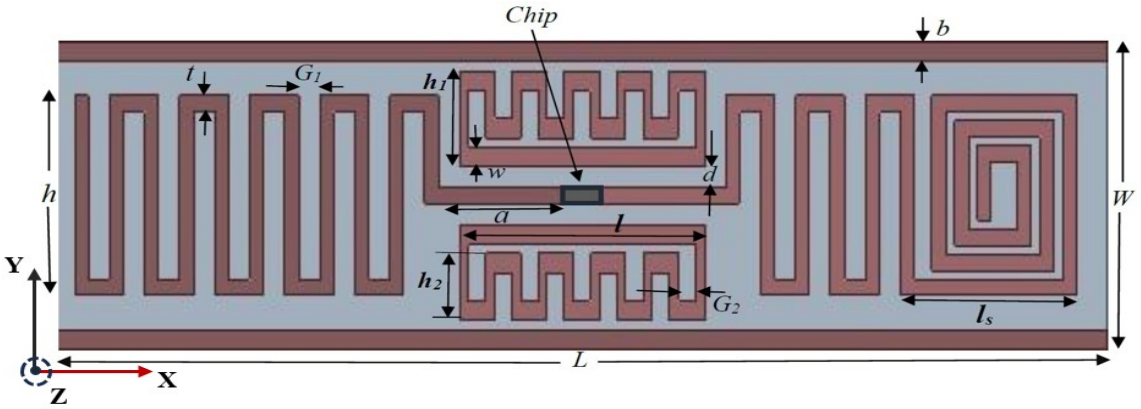

Figure 4.1: Schematic of the proposed antenna

height, gap, feed line and the MIL separation and thus, tag-chip impedance matching is validated on the desired frequency. The optimum values obtained for impedance matching is shown in Table 4.1.

The semiconductor-chip used in this article is Alien(Higgs-4) tag chip, which is having the reading sensitivity of -18.5 dBm. The internal RC circuit schematic of the microchip Alien Higgs used in this article is shown in Figure 4.2. The semiconductor chip is having complex impedance of $20.53 - j190.95\Omega$ at 866 MHz. The internal impedance of semiconductor-chip is obtained by formula:

Table 4.1: Numerical Values Of optimized Parameters Of Tag Antenna

Parameter	Value in mm	Parameter	Value in mm
L	60	W	16
a	7.2	l_s	10.1
w	1	b	1
h_1	5	G_2	1
G_1	1.2	d	0.8
t	0.8	l	14
h	10.4	h_2	3.5

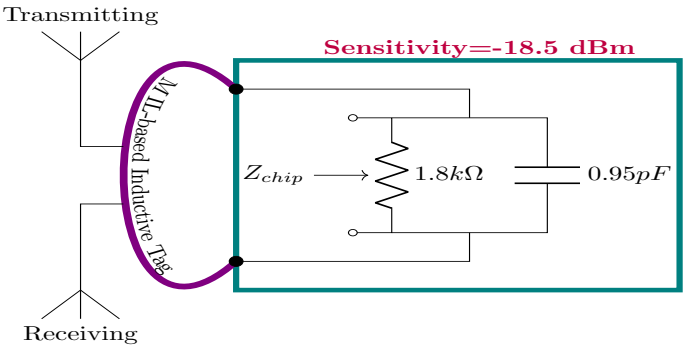

Figure 4.2: ALLIEN Higgs-4 IC application diagram

$$Z_{chip} = \frac{R}{1 + 4\pi^2 f^2 R^2 C^2} - j\frac{2\pi f R^2 C}{1 + 4\pi^2 f^2 R^2 C^2} \tag{4.1}$$

It is mandatory in scheming RFID tag that tag antenna impedance should be complex conjugated to that of semiconductor-chip for maximum power transfer. This matching is done through the binary states namely matched state and shorted state. Whenever tag antenna is matched with semiconductor-chip, the signal sent from reader is engrossed by the transducer and consequently semiconductor-chip changes to shorting state. In this state, tag antenna re-transmits interrogator signal to reader. The input impedance matching of the tag antenna with semiconductor-chip is displayed in Figure 4.7(f). The obtained impedance of the tag at 866 MHz is $20.62 + j190.94\Omega$. The reflection coefficient is reckoned by following formula in Eq. 4.2:

$$\Gamma_{tag} = \frac{Z_{chip} - Z_T^*}{Z_{chip} + Z_T} \tag{4.2}$$

where Z_{chip} and Z_T are semiconductor-chip and tag input impedance respectively, where Z_T= $R_T + jX_T$ and $Z_{chip} = R_C - jX_C$.

The tag antenna comprises two-sided MIL, which is inductively coupled with spiral ending meandered line. After combining spiral-ending meandered line and the Meandered-inductively loop, both terminals are attached to the semiconductor-chip. The equivalent circuit of this Meandered-inductively coupled loop antenna is displayed in Figure 4.3. Tag

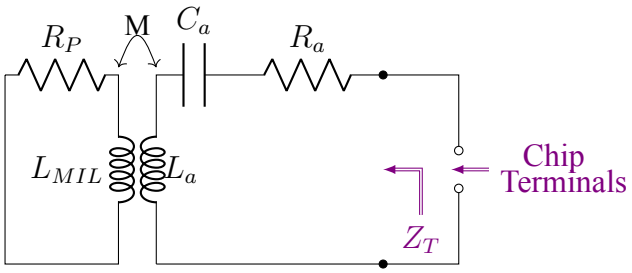

Figure 4.3: Spiral-ending meandered line with Meandered Inductive Coupled loop equivalent circuit

impedance of the presented MIL based antenna is given by [51],

$$Z_T = R_T + jX_T = Z_{MIL} + \frac{(2\pi f M)^2}{Z_a} \tag{4.3}$$

where Z_a and Z_{MIL} are impedances of spiral-ending meandered line and MIL respectively. M represents mutual inductance between the inductances. Z_a is calculated by:

$$Z_a = R_{a,0} + jR_{a,0}Q_a\left(\frac{f}{f_0} - \frac{f_0}{f}\right) \tag{4.4a}$$

where Q_a is quality factor and f_0 is the resonating frequency.

$$Z_{MIL} = R_P + j2\pi f L_{MIL} \tag{4.4b}$$

By putting values of Z_a and Z_{MIL} from (4.4a) and (4.4b) in (4.3) :

$$R_T = R_P + \frac{(2\pi f M)^2}{R_{a,0}\left(1 + \left[Q_a\left(\frac{f}{f_0} - \frac{f_0}{f}\right)\right]^2\right)} \tag{4.5a}$$

$$X_T = 2\pi f L_{MIL} - \frac{(2\pi f M)^2 Q_a \left(\frac{f}{f_0} - \frac{f_0}{f}\right)}{R_{a,0}\left(1 + \left[Q_a\left(\frac{f}{f_0} - \frac{f_0}{f}\right)\right]^2\right)} \tag{4.5b}$$

At resonating frequency of tag antenna, the resisistance and reactance values of input impedance of inductively coupled tag can be given by:

$$R_{T,0} = R_T\left(f = f_0\right) = R_P + \frac{\left(2\pi f_0 M\right)^2}{R_{a,0}} \tag{4.6a}$$

$$X_{T,0} = X_T\left(f = f_0\right) = 2\pi f_0 L_{MIL} \tag{4.6b}$$

Now, values of $R_{a,0}$, Q_a and M can be calculated by given formula:

$$R_{a,0} = \eta\pi\left(\frac{P}{\lambda_0}\right)^2\left\{\frac{\lambda_0}{P}\sum_{m=0}^{\infty} J_{2m+3}\left(\frac{2P}{\lambda_0}\right)\right\} \tag{4.7a}$$

where P is perimeter of loop antenna and λ_0 is wavelength at resonance frequency and summation part represents a series of Bessel functions.

$$Q_a = \frac{2\pi f_0 L_a}{R_a} \tag{4.7b}$$

$$M = \frac{\mu_0 l}{2\pi}\ln\frac{h_1 + d}{d} \tag{4.7c}$$

The inductance of the meander-line obtained by[50]:

$$L_m = 0.2l\left[0.022\left(\frac{w+t}{l}\right) + \ln\left(\frac{l}{w+t}\right) + 1.19\right] nH/mm \tag{4.8a}$$

where *l* is absolute meander-line length in mm, *t* is thickness in mm and *w* is width in mm. The self inductance of a straight filament of any rectangular section is given by[66]:

$$L_f = \frac{\mu_0}{2\pi} l\left\{\ln\left(\frac{2l}{w+w'}\right) + 0.50049 + \left(\frac{w+w'}{3l}\right)\right\}/10^3 nH \tag{4.8b}$$

where, *l* is the length of filament, *w* is breadth and *w'* is the thickness in mm. The meandered inductively-coupled loop inductance is calculated by parallel combination of the

both aforementioned inductance.i.e.:

$$L_{MIL} = L_m || L_f \tag{4.9}$$

By using above formulas, tag antenna impedance is calculated.

The analogous RLC circuit model of proposed antenna is shown in Figure 4.4. The antenna structure can be split into four parts in series i.e. spiral element, meandered antenna, MIL and the tag semiconductor microchip.The spiral network introduces capacitance in series with meandered line capacitance, hence capacitive reactance reduces and inductive part of the tag impedance increases and thus the conjugate impedance matching is attained with the semiconductor-chip.

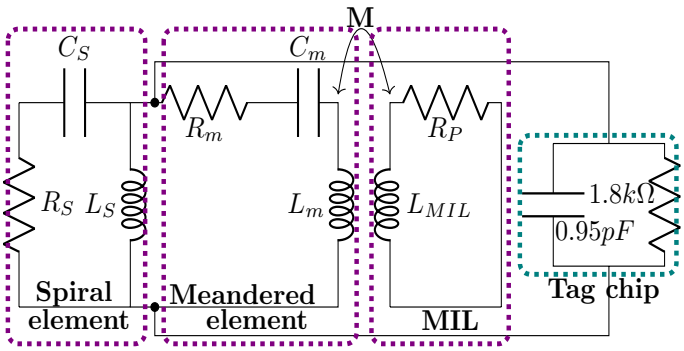

Figure 4.4: Equivalent circuit prototype of the proposed tag structure

The tag impedance is obtained at each frequency of UHF band and the reflection coefficient is calculated from Eq. 4.2 in that frequency range. The reflection coefficient for this tendered tag is displayed in Figure 4.5.

Design Considerations and Parameter Initialization: The tag antenna was designed to operate at 866 MHz, beginning with a simple rectangular loop structure. A meandering technique was applied for size reduction, while an inductively coupled loop was used to achieve impedance matching with the Higgs-4 chip. Starting values for trace width, gap (d), and loop height (h) were estimated from equivalent circuit models and refined through full-wave simulation. Each design iteration was evaluated based on impedance convergence and return loss, as shown in Fig. 4.7 and 4.8. The finalized dimensions formed the base for parametric analysis.

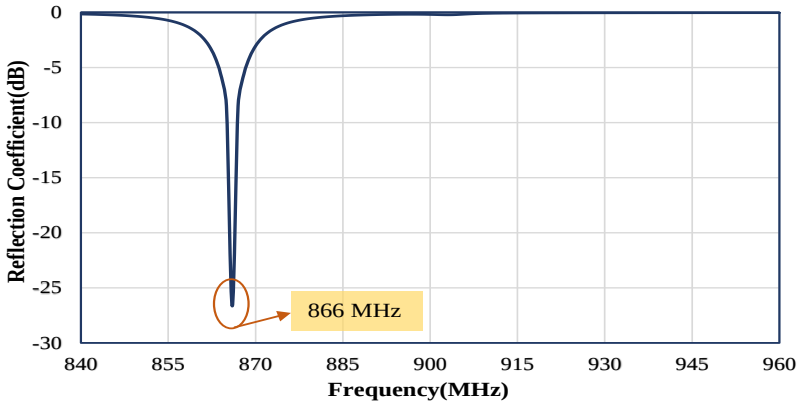

Figure 4.5: Reflection Coefficient of the UHF RFID tag antenna

4.3 Evolution Steps

The evolution steps to achieve final tag design is shown in Figure 4.6. Antenna I shows the meander-line tag, Antenna II shows spiral ending tag, Antenna III represents hybridization of previous two which is spiral-ending meandered line tag. Antenna IV represents both sides spiral-ending with Meandered Inductively-coupled loop(MIL) tag, Antenna V is obtained by introducing MIL in Antenna III and Antenna VI represents the final structure of designed RFID tag which is achieved by the metallization of the previous tag on top as shown in Figure 4.6(f).

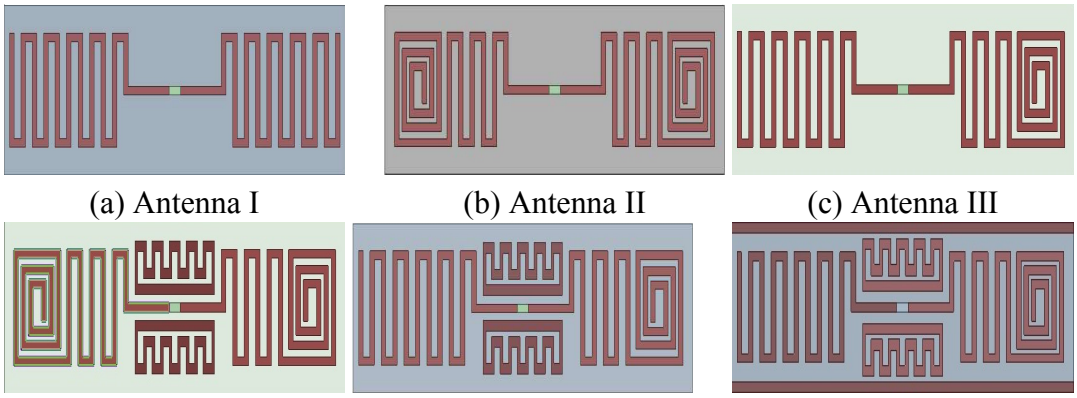

(a) Antenna I (b) Antenna II (c) Antenna III

(d) Antenna IV (e) Antenna V (f) Antenna VI

Figure 4.6: Evolution steps of this presented tag

The impedance matching graph of every step is shown in Figure 4.7.

From Figure 4.7(a), it can be seen that for Antenna I, the reactance of tag matches with semiconductor at 1331MHz while resistance matching is achieved at 1040 MHz. This tag is not inductive in nature in the UHF band of RFID. For the impedance matching of tag to

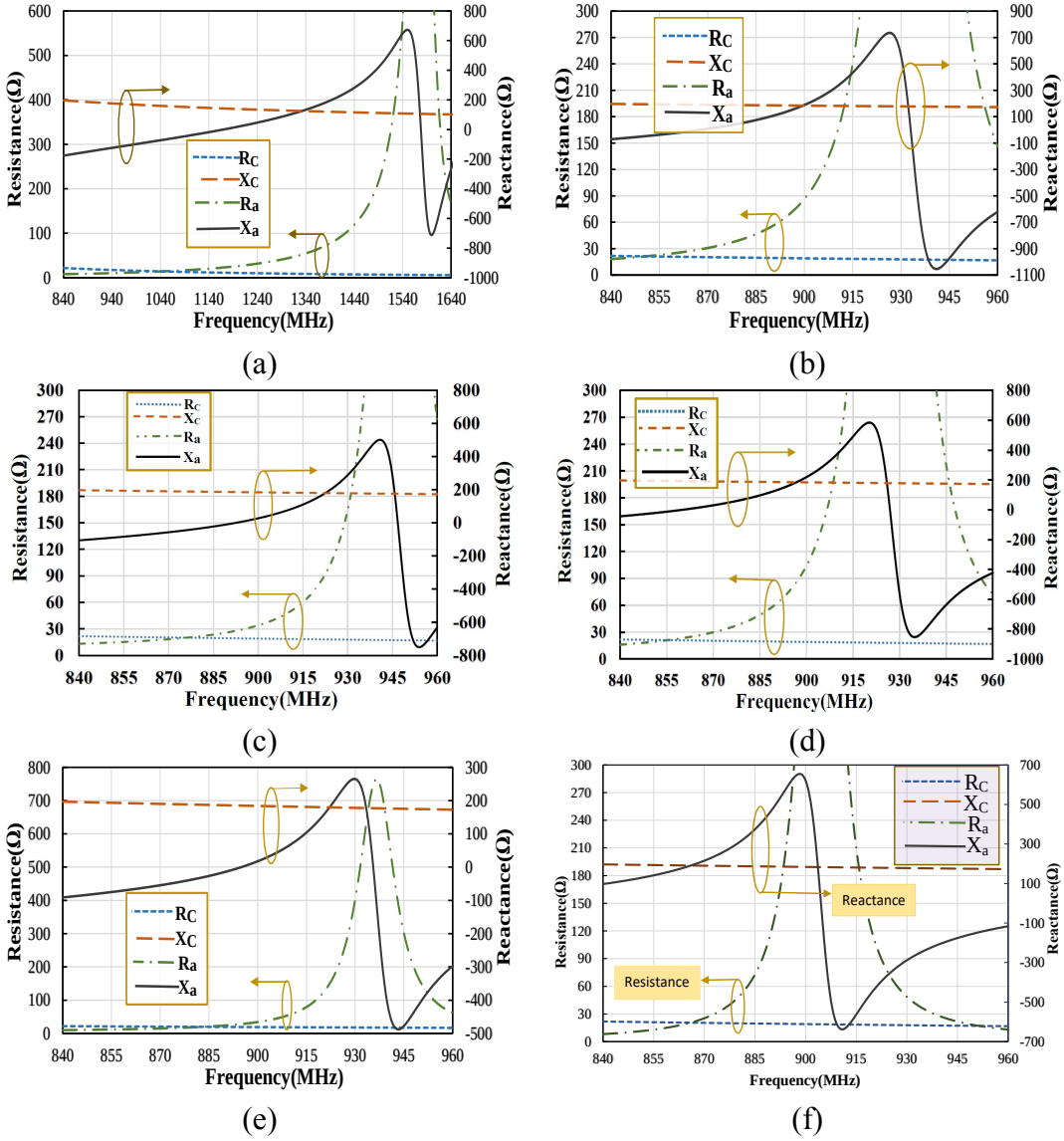

Figure 4.7: Input Impedances of every steps;(a) Antenna I-Complex Impedance(b) Antenna II-Complex Impedance,(c) Antenna III-Complex Impedance,(d) Antenna IV-Complex Impedance,(e) Antenna V-Complex Impedance,(f) Antenna VI-Complex Impedance

ASIC, tag needs to be inductive in the operating band of frequency. After putting spirals at the end of the tag, resistance and reactance both increases for the lower frequencies and thus tag becomes inductive in the range of 868 MHz to 933 MHz. For Antenna II, reactance matching happens at 899 MHz while that of resistance happens at 849 MHz. Thus there is 50 MHz of frequency gap. This gap reduces to 46 MHz after hybridization of previous two antennas as shown in Figure 4.7(c). Antenna III reactance part equals to that of ASIC at 922 MHz while resistance matches at 876 MHz. This hybridization lowers the resistance and reactance of tag for lower frequencies. Now, after putting MIL in Antenna II, this tag is again inductive for same frequency band-range but it is inductive in the range of 861 MHz to 926 MHz. The resistance matching happens at 855 MHz while same happens for reactance at 897 MHz. Thus the matching gap reduces to 42 MHz. Further, putting MIL in Antenna III, reactance part matches to ASIC at 923 MHz and same happens for resistance at 883 . Hence, the gap reduces to 40 MHz. Finally, after putting metal bar on both sides of Antenna V, this introduces high inductive impedance and impedance matching happens at 866 MHz with impedance of 20.62+j190.94Ω as shown in Figure 4.7(f).

4.4 Parametric Analysis

Different outcome on reflection coefficient and impedance is produced by every single parameter of proposed antenna. Parametric scrutiny is done by changing single parameter at a time and keeping others constant to check those effects. The impact of alteration of meander line height(h) and meandered-inductive loop separation from feed line(d) on input impedance and reflection coefficient is investigated. Variation of h elaborates effect of meander line and variation of d indicates effect of MIL separation from feeding line on impedance matching.

To evaluate response of height of the meander line and return loss on input impedance, tag is simulated by altering parameter h from 10.4mm to 11.2mm while retaining others constant. It is comprehended from Figure 4.8(a) that both real and imaginary parts match

with respective values of semiconductor-chip at lower frequency as *h* increases. Also, we can see impedance value increases as *h* increases at 866 MHz. When h is 10.4mm, we see the real part of impedance matches on 866 MHz with the semiconductor-chip reactance while the same happens for imaginary part on 874 MHz. Hence matching difference is found to be 8 MHz and tag antenna resonates at 874 MHz with poor reflection coefficient.

For $h = 10.8mm$, it is perceived that antenna resonates at 866 MHz.When $h = 11.2mm$,

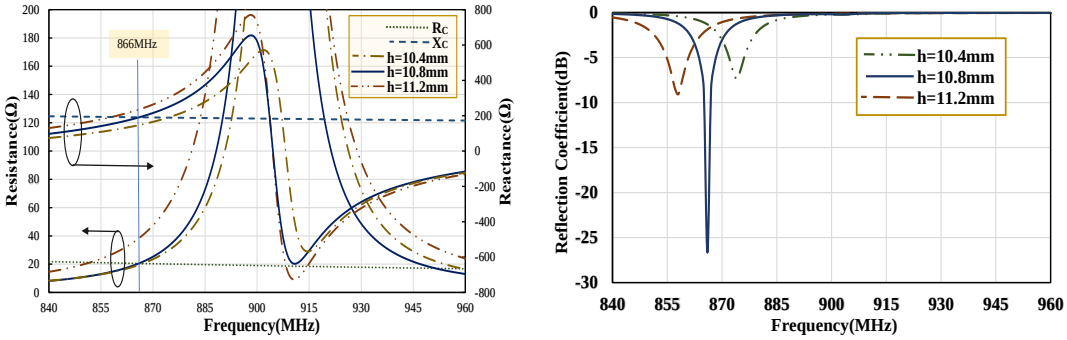

(a) (b)

Figure 4.8: (a) Simulated input impedance and (b) Reflection Coefficient after variation of h.

we see the real part of impedance matches on 851 MHz with microchip resistance at 851 MHz while the same happens for imaginary part on 858 MHz. For this value, matching difference is found to be 7 MHz and tag antenna resonates at 858 MHz with poor reflection coefficient. Reflection coefficient for above values of h is displayed in Figure 4.8(b). Thus, optimum value of h is found to be 10.8mm.

For investigating the impact of d on performance of this RFID antenna, it is altered from 0.4mm to 1.2mm while retaining others constant.

It is comprehended from Figure 4.9(a) that both real and imaginary parts match with respective values of semiconductor-chip at higher frequency as *d* increases. Also, we can see impedance value decreases as *d* increases at 866 MHz. When d is 0.4mm, impedance matching for real part happens at 859 MHz while that of imaginary part happens at 863 MHz. Thus we find the difference between matching is 4 MHz and tag antenna resonates at 874 MHz with poor reflection coefficient.When $d = 1.2mm$, matching of real part of tag antenna happens at 865 MHz while that of reactance happens at 867 MHz. At this value the difference is 2 MHz and antenna resonates at 867 MHz with poor reflection

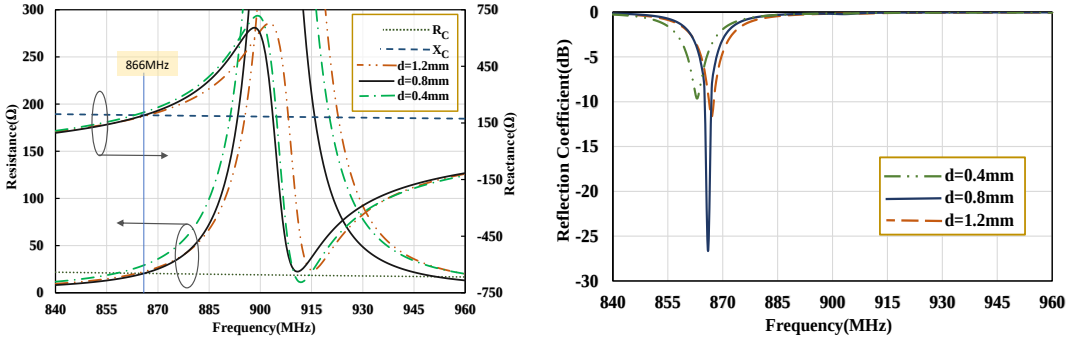

(a) (b)

Figure 4.9: (a) Simulated input impedance and (b) Reflection Coefficient after variation of d.

coefficient. Reflection coefficient for above values of d is displayed in Figure 4.9(b). Thus, from Figure 4.9, it is noticed that optimum reflection coefficient is achieved for $d = 0.8mm$.

4.5 Results and Discussion

Prototype of fabricated meandered inductive-coupled loop RFID tag antenna with FR4 substrate is shown in Figure 4.10. The measurement setup with Vector Network Analyzer is displayed in Figure 4.11.

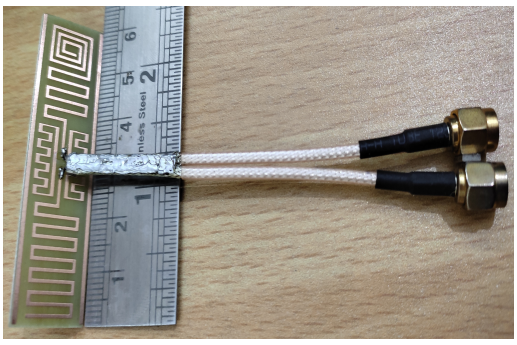

Figure 4.10: Fabricated proposed RFID tag antenna with differential-probe

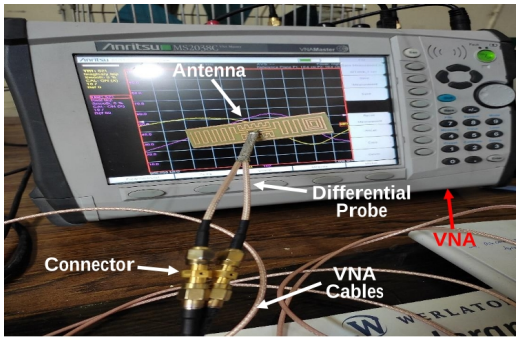

Figure 4.11: Measurement of UHF Tag

The Scattering-parameters of this proposed antenna were measured by Anritsu(MS2038C) VNA and then by using subsequent formula, the differential input impedance (Z_{diff}) of

tag antenna is calculated.

$$Z_{diff} = 2Z_0 \frac{(1 + S_{12}S_{21} - S_{11}S_{22} - S_{12} - S_{21})}{(1 - S_{11})(1 - S_{22}) - S_{21}S_{12}} \tag{4.10}$$

The simulated and measured impedance and reflection coefficient of UHF tag is displayed in Figures 4.12 and 4.13 respectively. The measured input impedance is $20.6 + j190.9\Omega$ at 866 MHz, that is almost complex conjugate to semiconductor-chip impedance.

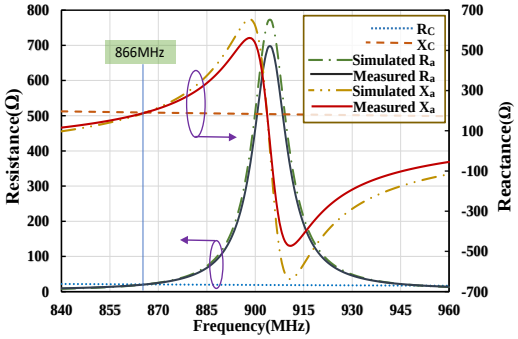

Figure 4.12: Measured amd simulated input impedance of tag antenna

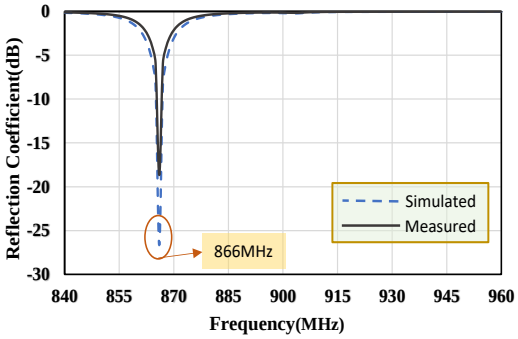

Figure 4.13: Measured and simulated reflection coefficient of RFID tag

Figure 4.14 shows the radiation pattern of proposed antenna at 866 MHz. It can be seen that this antenna produces a good radiation performance and attains quasi-isotropic radiation pattern and looks analogous to that of dipole.

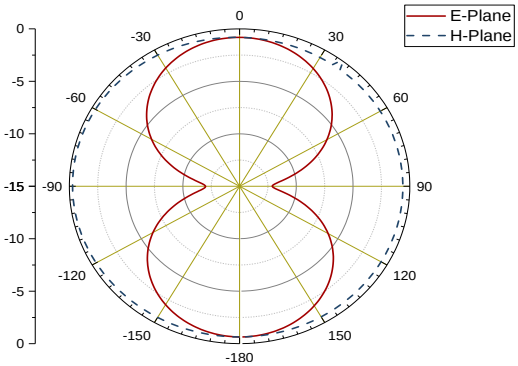

Figure 4.14: Far-field radiation pattern for E-plane and H-plane at 866 MHz

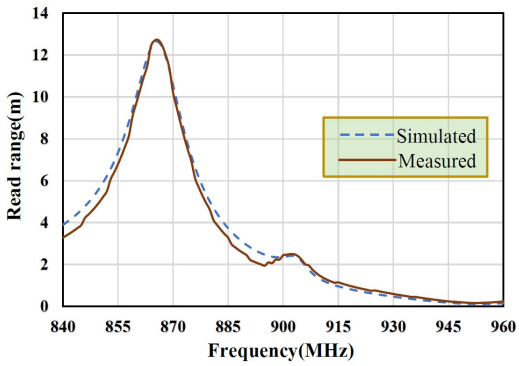

Figure 4.15: maximum separation between reader and tag

The maximum possible separation between reader and tag for switching-on semiconductor-chip i.e. read range is given by the formula given in Eq. 4.11.

$$S_{max}(\theta, \phi) = \frac{\lambda}{4\pi} \sqrt{\frac{EIRP_R}{P_{th,chip}} (1 - |\Gamma|^2) G_t(\theta, \phi)} \tag{4.11}$$

where $G_t(\theta, \phi)$ represents gain, Γ is voltage reflection coefficient and $(1 - |\Gamma|^2)$ is power transmission coefficient. The tag is evaluated for 4W EIRP reader.

The $G_t(\theta, \phi)$ is further expressed by,

$$G_t(\theta, \phi) = (1 - |\Gamma|^2)\eta_{cd}D \tag{4.12}$$

where, η_{cd} is the radiation efficiency, D is directivity.

The maximum separation between tag and reader, obtained from Eq. 4.11, is plotted in Figure 4.15. The tag read range attains its maximum value upto 12.6 meters at 866 MHz. At airports, luggage orientation can change, so circularly polarised antenna is installed in RFID reader. Since, Proposed tag antenna is linearly polarised along the X-direction (along the antenna's length) and radiation pattern is bidirectional with significant read range, this tag antenna is applicable at airports for luggage tracking irrespective of reader orientation.

Table 4.2 analyzes an analogy between this work and other preceding communicated

Table 4.2: Distinct parameters correlation of the tendered antenna with few preceding communicated antennas

Antenna	**Dimensions (mm^3)**	**Antenna substrate**	**Chip Sensitivity (dBm)**	**Frequency (MHz)**	**% Size reduction**	**Read range(m)**
[67]	$67 \times 16 \times 1.54$	FR4	-20.5	866	6.96	10.2
[68]	$66 \times 20 \times 1.6$	FR4	-17.4	867 & 956	27.27	5
[69]	$60 \times 20 \times 1.6$	FR4	-20	866 & 912	20	5.5
[60]	$31.5 \times 31.5 \times 3.2$	PP4 foam	-17.8	867	51.6	7.25
[40]	$91 \times 91 \times 1.6$	FR4	-17.4	866 & 952	88.4	3
[70]	$128 \times 50 \times 1.6$	FR4	-16	866 & 915	85	6.8
[71]	$120 \times 60 \times 1.6$	Rogers RT/duroid	-18.5	865	86.67	13.9
Proposed work	$60 \times 16 \times 1.6$	FR4	-18.5	866	-	12.6

antennas w.r.t. identical operational band in terms of dimensions, used antenna substrate, chip sensitivity, reduction in size and reading territory. This correlation is done for particular UHF tags which were operated in the same proximity of frequency of operation, also antenna material used are same as that of the proposed antenna except [60] and [71].

Although, this tag antenna has lower read range compared to [71], yet it has 86.67% size reduction. The size reduction percentage shown in Table 4.2 is for proposed tag antenna relative to corresponding referenced antenna. It can be seen that by using meandered dipole, admirable size reduction is achieved. In spite of being tiny tag antenna, this tag antenna provides higher tag-reader separation distance.

4.6 Outcome

In this article, a novel meandered dipole with spiral end is produced. The antenna impedance is conjugately-matched to Alien Higgs semiconductor-chip of power sensitivity of -18.5 dBm for the maximum power transfer. The equivalent circuit of the tendered antenna is analysed with equations. The Proposed RFID tag antenna is operated at 866 MHz. Further, an enhanced reading-territory is obtained. This tag antenna advances its tag to reader length upto 12.6 meters, which makes it applicable for luggage tracking at airports.

Following Chapter 4's insights into compact and inductively matched antennas operating at 866 MHz, Chapter 5 integrates multiple matching techniques, including combined Nested Slot and inductive coupling, to maximize both size efficiency and read range. Operating in the 902-928 MHz regulated UHF band (resonating at 902 MHz), this design achieves a detection range exceeding 14 meters, making it suitable for long-range RFID applications. This chapter's work exemplifies a balance between miniaturization and extended read range, meeting the demands of high-performance applications.